ACS OMEGA

http://pubs.acs.org/journal/acsodf

Article

Synergistic Effect of Chitosan and Metal Oxide Additives on Improving the Organic and Biofouling Resistance of Polyethersulfone Ultrafiltration Membranes

Herlambang Abriyanto, Heru Susanto,* Talita Maharani, Abdullah M. I. Filardli, Ria Desiriani, and Nita Aryanti

Cite This: *ACS Omega* 2022, 7, 46066−46078

Read Online

ACCESS | Metrics & More | Article Recommendations

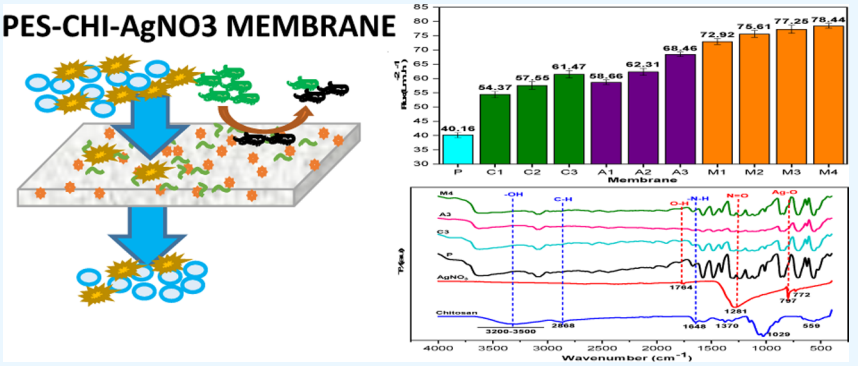

ABSTRACT: The combination of chitosan and metal oxides was utilized as an addition to improve the fouling resistance of polyethersulfone (PES) ultrafiltration membranes. Pure water flux, membrane hydrophilicity by the contact angle, scanning electron micrographs, and Fourier-transform infrared spectra were used to characterize the membranes. With the addition of metal oxides, the modified membrane's water flux increased. The PES membrane with 0.25% wt chitosan and 2.0% wt $AgNO_3$ had the highest flux and antibacterial activity among the membranes tested. Because of its potential to improve membrane hydrophilicity, the water flux increased with the addition of chitosan and $AgNO_3$. Because of the improved hydrophilicity, the contact angle reduced as chitosan and Ag loading was increased. The PES−chitosan−Ag_2O (from $AgNO_3$ 2.0% wt) membrane had high antibacterial activity against *Escherichia coli* and *Staphylococcus aureus*, whereas the PES−2.0% wt Ag membrane did not show the same result. Finally, the addition of chitosan in the PES−Ag membrane increased the membrane's antibacterial activity substantially.

1. INTRODUCTION

Many industries have been interested in applying ultrafiltration (UF) membranes to replace conventional separation and perform mass separation; such membranes can also be used as a pretreatment before reverse osmosis.[1,2] Process condition adjustment and membrane material selection determine the success of using UF membranes.[3] The membrane material determines various membrane specifications such as the hydrophilic nature, interfacial properties, and pH range, all of which have a direct impact on membrane performance such as permeability and selectivity.[4,5] However, fouling (organic and biofouling) is a significant issue in UF applications because it causes severe flux reduction and affects productivity.[6−8] Most UF membranes are fabricated from the polyethersulfone (PES) polymer.[9−11] PES features extreme pH resistance and outstanding thermal stability, hydrolytic properties, mechanical properties, and film-forming properties.[12] Despite this, PES's hydrophobicity can lead to severe organic fouling.[13] In addition, as a polymer, PES is prone to biofouling.[12]

Membrane fouling refers to the formation of particulates, colloidal matter, microbes, and macromolecules on the surface or within the pores of a membrane. Organic fouling and biofouling commonly occur in UF membrane applications. Organic fouling is caused by strong foulants of organic macromolecules, such as polysaccharides and proteins.[11,14,15] In addition to organic fouling, biofouling caused by microorganisms is also prominent. In this paper, biofouling is defined as the accumulation of biologically active organisms,

Received: June 13, 2022
Accepted: November 21, 2022
Published: December 6, 2022

https://doi.org/10.1021/acsomega.2c03685
ACS Omega 2022, 7, 46066−46078

such as microbes, extracellular biopolymers, fungi, and bacteria, on the membrane surface, which blocks or covers the pores of the membrane, resulting in the formation of new layers and a decrease in permeate flux or an increase in transmembrane pressure.[7,8,16] Biofouling occurs when bacteria or microorganisms attach on the membrane surface.[17] The first stage of membrane biofouling is determined by the foulant's capacity to bind to the membrane surface, which is influenced by hydrophobic interactions, covalent bonds, and electrostatic forces.[6,18,19] Therefore, to prevent or decrease biofouling, undesirable adhesion interactions between the foulant and the membrane must be avoided.[3] In most cases, fouling is exacerbated by the interaction of organic fouling and biofouling.[15]

Hydrophilicity and antimicrobial activity are important characteristics of membranes for fouling reduction. Several techniques have been proposed to obtain a hydrophilic surface with antifouling properties. Adsorption of appropriate hydrophilic polymers on the membrane surface can contribute to repulsion between the protein molecule and membrane surface.[20] Increasing the hydrophilicity of the membrane surface by blending with hydrophilic polymers,[21,22] coating,[10,23] and surface grafting[24,25] can effectively reduce irreversible membrane fouling. These strategies provide hydrophilic polymers to the membrane matrix directly or indirectly, enhancing the antifouling capabilities of the polymer membrane.[15]

The classic and most practical method for membrane alteration is to blend the polymer with additives. Direct mixing of additive macromolecules with the host membrane matrix to introduce their properties into the membrane polymer is one blending strategy. Some additives used in the blending technique are polyvinylpyrrolidone,[26,27] polyethylene glycol,[21,28] polyvinyl alcohol,[23,29] polyacrylic acid,[25,30] poly(sodium 4-styrenesulfonate),[24] polyethyleneimine,[31,32] Pluronics,[27] and chitosan.[22,33] Kumar et al.[33] found that chitosan can improve membrane performance. Chitosan solution can be used as a surface coating for non-woven fabric membranes to improve their antifouling qualities and inhibit protein degradation in UF membranes via immersion or flow-through methods.

Chitosan derivatives are less harmful and more biocompatible in nature than other organic or inorganic additives.[34,35] In our previous research, we developed a UF membrane modified using chitosan compound with Tween 80 and used this membrane to separate bovine serum albumin (BSA) proteins.[21] However, the application of chitosan in the membrane solution is limited by its high viscosity and low solubility; thus, only a small amount of chitosan could be added.[22] Consequently, the amount of chitosan included into the membrane matrix is also limited. In addition, the antibiofouling character could not be observed.

Pretreatment of feed water is a typical method for preventing microbial fouling of membranes.[3] This method reduced the amount of microbes and nutrients that microbes consumed in water.[17,36] However, such pretreatment is time-consuming and costly. Furthermore, even if microbes are removed from the feed stream with a 99.99% success rate, this does not guarantee the absence of microbe growth on the membrane because they can grow, reproduce, and migrate quickly.[37] As a result, other biofouling mitigation strategies are critical.

Metal oxides are commonly incorporated into the polymer membrane to improve antimicrobial activity. Some of the metal oxides used in membrane modification were MgO,[38] GO,[39,40] SiO_2,[41] ZnO,[42] and Ag_2O.[16,43] Ahsani et al. proved that polyvinylidene fluoride (PVDF) membranes with the Ag–SiO_2 metal oxide have stronger biofouling resistance than pure PVDF membranes.[43] Because of its catalytic, optical, and conductive properties, silver oxide has received a lot of attention.[8] Overall, metal oxide additives increase membrane performance. However, past studies have revealed significant disagreement, presumably due to the many variables involved, such as membrane polymer properties, the solvent employed, preparation conditions, and process conditions for performance testing. As a result, determining the best metal oxide additive is challenging.

Most previous studies found that efforts to increase UF membrane resistance to organic fouling were not followed by an increase in resistance to biofouling, or vice versa. In this study, the resistance of UF membranes to both organic fouling and biofouling was carried out simultaneously. The combination of chitosan and metal oxides was used as additives in the fabrication of PES UF membranes. The use of chitosan is expected to increase membrane resistance toward organic fouling and biofouling, while the use of metal oxides is expected to increase resistance toward biofouling. The performance of metal oxides was compared in a systematic way. All of the preparation conditions, including the concentration of the membrane casting solution, were maintained. Thereafter, the selected metal oxides were combined with chitosan as additives.

2. MATERIALS AND METHODS

2.1. Materials. The membrane was made of PES from Merck (Germany). The solvent was *N*-methyl-2-pyrrolidone (NMP) from Merck (Germany). As an additive, chitosan from Biotech Surindo (Indonesia) was used. Acetic acid was purchased from Merck (Germany). Tween 80 purchased from KAO Indonesia Chemicals (Indonesia) was used as the surfactant during chitosan dissolution. Silver nitrate ($AgNO_3$), magnesium oxide (MgO), zinc oxide (ZnO), and silicon dioxide (SiO_2) purchased from Merck (Germany) were used as inorganic additives. BSA was acquired from Agdia, Inc. (Elkhart, USA). Pure water used was produced using a homemade RO–ion exchange system. Potassium dihydrogen phosphate (KH_2PO_4) and sodium hydrogen phosphate (Na_2HPO_4) were phosphate buffer solution that was used to make BSA under acidic conditions. Sodium hydrogen carbonate ($NaHCO_3$) and sodium carbonate (Na_2CO_3) were carbonate buffer solution that was used to make BSA under alkaline conditions.

2.2. Experimental Methods. *2.2.1. Preparation of PES–Metal Oxide Membranes.* A PES–metal oxide dope membrane solution was prepared by dispersing various types of metal oxides (MgO, SiO_2, ZnO, and $AgNO_3$) into the NMP solvent and stirring for 3 h until the metal oxides were completely dispersed. Thereafter, the PES polymer was added slowly (until the concentration of PES was 13% wt) to the NMP–metal oxide dispersion and stirred until it completely dissolved at 70 °C. The solution was agitated for 24 h to ensure homogeneity and then left at room temperature overnight until no air bubbles were visible. The dope solution was then transferred upon a glass substrate to create a membrane sheet.

To create a membrane sheet, the dope solution is then applied to a glass substrate. The casting process is done at

https://doi.org/10.1021/acsomega.2c03685
ACS Omega 2022, 7, 46066−46078

Table 1. Composition of the Polymer, Chitosan, and Metal Oxide during the Preparation of the Composite PES UF Membrane

variable	code	PES	chitosan	$AgNO_3$	SiO_2	MgO	ZnO
PES 13% wt	#P	13					
$SiO_2$1.00% wt	#S	13			1.00		
MgO 1.00% wt	#M	13				1.00	
ZnO 1.00% wt	#Z	13					1.00
$AgNO_3$1.00% wt	#A1	13		1.00			
$AgNO_3$1.50% wt	#A2	13		1.50			
$AgNO_3$2.00% wt	#A3	13		2.00			
chitosan 0.15% wt	#C1	13	0.15				
chitosan 0.20% wt	#C2	13	0.20				
chitosan 0.25% wt	#C3	13	0.25				
chitosan 0.25% wt−$AgNO_3$0.50% wt	#M1	13	0.25	0.50			
chitosan 0.25% wt−$AgNO_3$1.00% wt	#M2	13	0.25	1.00			
chitosan 0.25% wt−$AgNO_3$1.50% wt	#M3	13	0.25	1.50			
chitosan 0.25% wt−$AgNO_3$2.00% wt	#M4	13	0.25	2.00			

room temperature which is 26 ± 1 °C and 60 ± 5% humidity. The membrane was made using the nonsolvent-induced phase separation (NIPS) process with a non-solvent compound in the form of distilled water. One liter of distilled water is put into a container, and the printed membrane is then mixed with distilled water so that the NIPS process takes place perfectly. After spending 24 h in distilled water, the membrane was removed, dried with a tissue, and then heated to 60 °C for 24 h to drive out any remaining water and solvent from the membrane pores. The membrane was cut according to the size of the Amicon 8010 cell model and cross-flow test equipment, and the membrane was stored in a watertight sealed plastic container.

2.2.2. Preparation of PES−Chitosan−Ag_2O Membranes. A PES−Ag_2O dope membrane solution was prepared by dispersing $AgNO_3$ into NMP and agitating for 3 h until the metal oxide was completely dispersed. Then, at 70 °C, PES (13% wt) was gradually added and agitated until it completely dissolved. To avoid air bubbles, the solution was agitated for 24 h to produce a homogeneous dispersion before being allowed to rest at room temperature overnight.[8] In another container, 4 g of chitosan was dissolved in 95.8 mL of 2% vol acetic acid. Then, Tween 80 was poured into the chitosan solution with a Tween 80 to chitosan ratio of 1:20.[11] The chitosan mixture was stirred until it was homogeneous. The chitosan solution was slowly mixed with the PES solution for membrane dope solutions, with chitosan 0.25% wt. Furthermore, the solution was preheated at 70 °C and stirred for 24 h. Table 1 shows the composition of the polymer, chitosan, and metal oxide during the preparation of the composite PES UF membrane.

2.3. Characterization. *2.3.1. Pure Water Flux.* A dead-end stirred filtering system with the Amicon 8010 cell model (Millipore) was used to assess pure water flux (PWF). To minimize the impacts of compaction, every membrane was compressed for at least 1 h before flux measurement by filtering pure water at four bars. The flow was computed in this manner

$$J = \frac{V}{A \times t} \quad (1)$$

where J is membrane PWF given in $L{\cdot}m^{-2}{\cdot}h^{-1}$ and V is the volume permeate collected over time (t) using a membrane area of A (m^2).

2.3.2. Contact Angle. The surface hydrophilic nature of the membrane was examined using the contact angle (CA). OCA 25 from DataPhysics Instrument GmbH, Germany, was used to measure the static sessile drop CA. Using a syringe, 5 μL of water was dropped onto the membrane surface. Five to 10 random dropping spots on the membrane surface were employed to determine the membrane CA to minimize measurement error.

2.3.3. Membrane Functional Groups. Fourier-transform infrared (FTIR) spectroscopy was used to examine the functional groups of membranes. The membrane samples' FTIR spectra were acquired in the wavenumber range of 400−4000 cm^{-1} using a PerkinElmer/Spotlight 400 Frontier (USA) spectrometer. In the sample tested, the number of points was 3601 with the data interval −1. The number of scans performed was three with a resolution of 4.

2.3.4. Membrane Morphology. The morphology of surface and cross-sectional membrane pictures was examined using scanning electron microscopy (SEM) (Phenom Pro X desktop SEM, the Netherlands). Gold nanoparticles were sputter-coated onto the membrane samples. Before visualization, the membranes received a gold coating. During cross-section analysis, the membrane was cut in liquid nitrogen. The type of detector used in this analysis is the backscattering electron detector. Surface SEM is performed with a 10,000 times magnification, while the SEM cross-section is done with a magnification of 1000 times.

2.4. Performance Examination. *2.4.1. Antibacterial Properties of the Membrane.* The inhibitory zone approach was used to assess the membrane's biofouling resistance. By filling the filter sheets with antibiotic discs, the membrane and control samples were impregnated. Under sterile conditions, suspensions containing *Escherichia coli* or *Staphylococcus aureus* were inoculated on agar plates. On top of the agar, membrane samples and control discs were carefully deposited. The establishment of an inhibitory growth zone was seen after 24 h of incubation at 37 °C for *E. coli* or *S. aureus*. The shape of membranes used in the antibacterial test is a circle with a diameter of 8 mm which has an area of 50.24 mm^2.

2.4.2. Adsorptive Fouling. The equipment used for the adsorptive fouling test was the same as that in the previous experiment for PWF measurements. The method for adsorptive fouling followed our previous publication.[11] In brief, the membrane sample was compacted for at least 1 h. Following this, at a pressure of 4 bars, the PWF was observed.

https://doi.org/10.1021/acsomega.2c03685
ACS Omega 2022, 7, 46066−46078

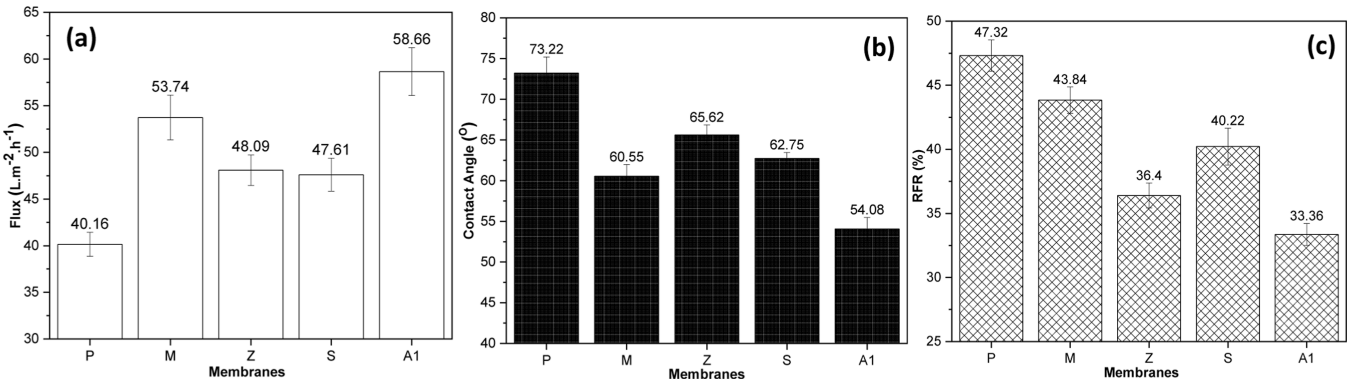

Figure 1. Membrane PWF (a), CA (b), and RFR after adsorptive fouling (c).

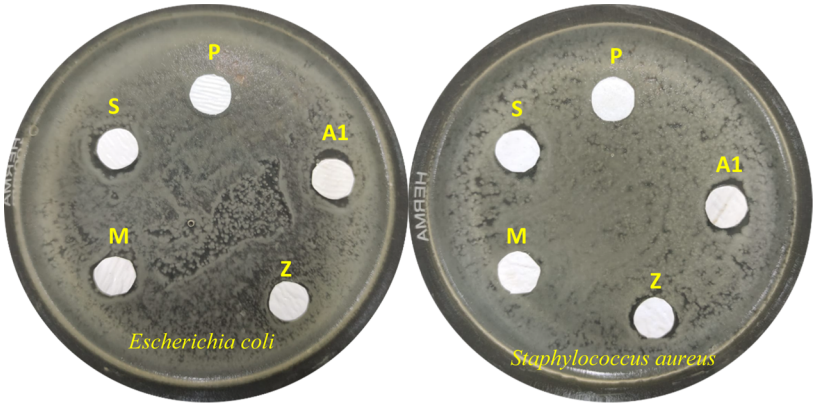

Figure 2. Disk diffusion tests for *E. coli* and *S. aureus* on the PES membrane containing metal oxides.

The cell was then emptied and filled with 1 g/L BSA solution, and the membrane surface was subjected to no flux for 3 h at a 300 rpm stirring rate. After this, the BSA solution was removed, and the membrane surface was rinsed. The flux after adsorption was then measured. Evaluation of the tendency to adsorb fouling is explained using relative flux reduction (RFR) with eq 2.

$$\%\ \mathrm{RFR} = \frac{J_O - J_a}{J_O} \times 100 \tag{2}$$

2.4.3. Cross-Flow UF. The performance of the cross-flow UF process was evaluated using a laboratory-scale cross-flow filtration apparatus. The membrane sample was compacted first by filtering pure water at 3.5 bars for 30 min and then gradually lowering the pressure to 3.5 bars. The PWF was measured once the pressure was steady, and the pure water was replaced with BSA solution (0.1 g/L). The BSA solution used has two pH values: an acidic pH of 5 and an alkaline pH of 8. Phosphate buffer solution (KH_3PO_4 and Na_2HPO_4) was used to make BSA under acidic conditions, and carbonate buffer solution was used to make BSA under alkaline conditions ($NaHCO_3$ and Na_2CO_3). Gravimetrically, the flux profile (expressed in terms of normalized flux, J/J_O) through time was observed. To maintain a steady feed concentration, the volume of feed should be substantially bigger than the volume obtained as a sample for analysis. Furthermore, the retentate and permeate were reintroduced into the feed tank.

2.4.4. Membrane Surface Charge Analysis. The membrane surface charge was characterized by measuring the streaming potential using a homemade apparatus. The experimental setup and the method were similar to those in our previous publication.[44]

2.4.5. Membrane Stability Analysis. A stability test was carried out to determine the durability of the membrane in water for a long time. The membrane was shaken at a speed of 100 rpm at a temperature of 28 °C while being submerged in distilled water for 21 days in a closed Erlenmeyer tube. The dripping water was then taken as much as 20 mL for an X-ray fluorescence (XRF) test (Rigaku NEX QC EDXRF, Japan) to determine whether the Ag compound was released into the water. The membrane was extracted and dried in an oven at 60 °C for 24 h to get rid of the water content in the membrane pores. The membrane was then examined using SEM to determine the Ag compounds still present on the membrane matrix's surface. In order to establish that Ag is still present on the membrane's surface, which can confer antibacterial capabilities on the membrane, the stability of the membrane under examination is also put through another antibacterial test, while for membranes containing chitosan, the soaked membranes were then dried and tested by FTIR.

3. RESULTS AND DISCUSSION

3.1. Metal Oxide Selection. *3.1.1. PWF and Water CA.* Some metal oxides were evaluated and selected. The selection of metal oxides was determined by measuring their PWF, hydrophilicity (CA), and adsorptive fouling resistance. RFR was measured to express adsorptive fouling. The higher the RFR, the more the adsorptive fouling occurs. The results are shown in Figure 1. Regardless of the metal oxide type, the addition of metal oxides increased the PWF of the PES membrane. The highest increase in PWF was demonstrated by

https://doi.org/10.1021/acsomega.2c03685
ACS Omega 2022, 7, 46066−46078

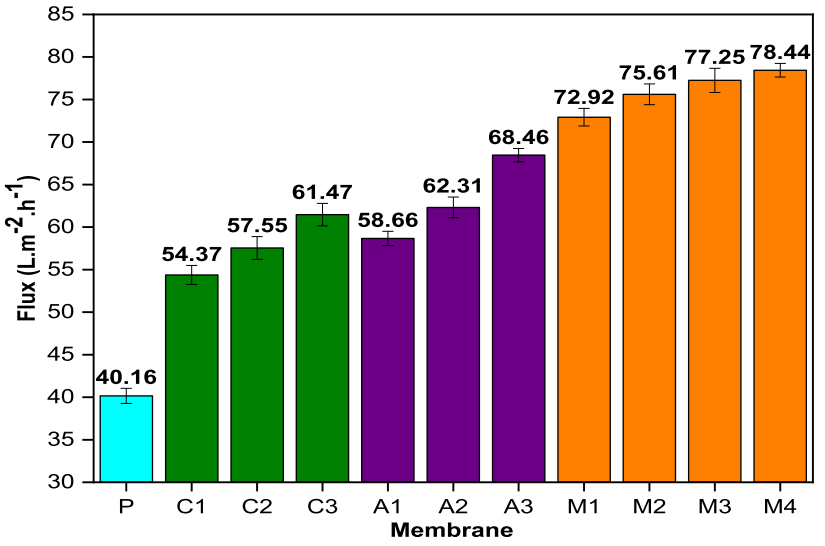

Figure 3. PWF of the PES−chitosan−Ag_2O membrane.

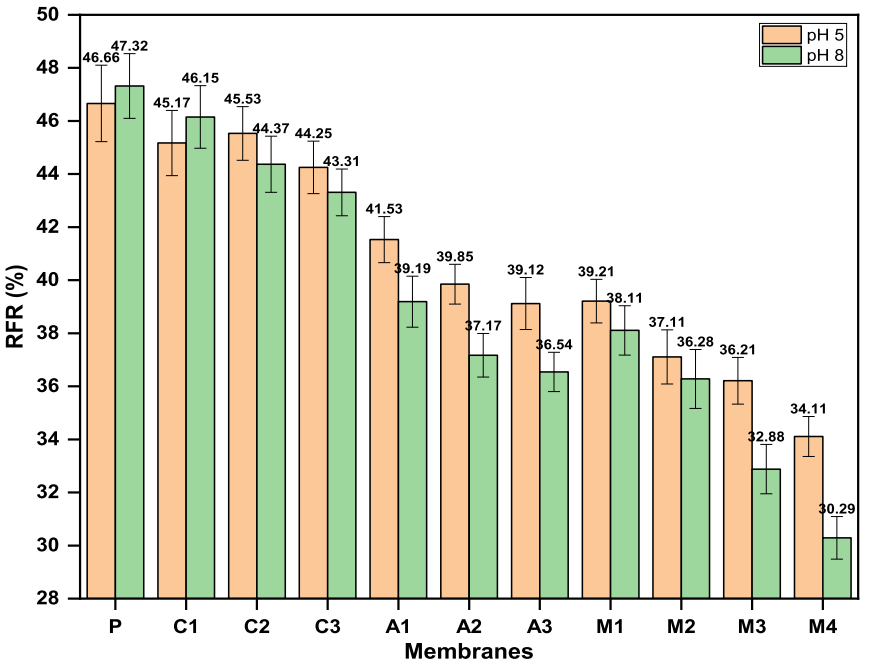

Figure 4. RFR of the chitosan−$AgNO_3$ membrane.

the addition of $AgNO_3$. Compared with the PES (only) membrane, the addition of $AgNO_3$ (1% wt) increased PWF by ∼46%. The water CA was significantly reduced by the addition of metal oxides, with $AgNO_3$ showing the greatest reduction followed by MgO, SiO_2, and ZnO. The membrane's hydrophilicity rises as the CA decreases. This hydrophilicity helps the membrane's PWF in addition to the pore structure. It is important to inform that because the silver in the PES membrane was in the form of silver oxide (see Section 3.2.9), the PES membrane prepared with the addition of $AgNO_3$ is expressed as PES−Ag_2O.

Adsorptive fouling studies with BSA solution demonstrated that the PES (only) membrane showed the highest RFR, indicating that it is most prone to protein fouling adsorption. By contrast, the addition of $AgNO_3$ resulted in the PES UF membrane having the highest fouling resistance toward protein fouling. Overall, the order of membrane resistance toward adsorptive fouling was PES < PES−MgO < PES−SiO_2 < PES−ZnO < PES−Ag_2O. These results agree well with the hydrophilic character of the membranes and with previous studies by other authors.[45−47]

3.1.2. Antibacterial Activities in Membrane Nanoparticles. Antibacterial examination was conducted by a zone of inhibition (ZoI) test (Figure 2). The membrane with nanoparticle additives showed antibacterial activity, as indicated by the presence of a ZoI around the membrane. By contrast, the PES membranes without metal oxides did not show any ZoI, and bacteria grew on the surface of the membrane. The hydrophobic characteristic of the PES polymer was the primary cause of microorganism attachment and proliferation on the membrane surface.

The value of the ZoI area formed on each membrane with *E. coli* bacteria is 32.992, 12.087, 19.696, and 28.321 mm^2 and for *S. aureus* bacteria is 23.052, 14.200, 7.699, and 18.851 mm^2 for

https://doi.org/10.1021/acsomega.2c03685
ACS Omega 2022, 7, 46066−46078

the A1; Z; M; and S membrane. Metal oxides in PES membranes have been shown to limit bacterial growth, implying that metal oxides are important in improving the antibacterial activity of PES membranes. The membranes' antibacterial effectiveness is based on their ability to degrade the bacterial cell wall. The interaction of the positive and negative charges in microbial cells is related to antibacterial activity. Metal oxides were thought to penetrate bacterial cell membranes and restrict bacterial proliferation by attaching tightly to cell contents, causing bacterial lipids, proteins, and DNA to be damaged. It causes bacterial cell death by disrupting the cell wall.[47] Metal oxides also have photocatalytic characteristics,[48] which enable them to produce reactive oxygen molecules and destroy organic substances, including bacteria.

Comparison of the antimicrobial activity of the metal oxides used revealed that Ag_2O exhibited the highest resistance toward biofouling, followed by ZnO, SiO_2, and MgO. The antimicrobial activity of Ag_2O has been explained in the previous publication.[49] In brief, Ag_2O adherence to the bacterial cell membrane increases permeability and interferes with respiration. It can destroy the disulfide bonds of bacteria to resist the synthesis of bacterial cells. Ag metal oxides are often loaded on suitable carriers, which effectively prevent aggregation and help develop their antibacterial properties.[49] Overall, results showed that the metal oxides used in this study demonstrated antimicrobial activity, indicating that they were good additives against biofouling. Regardless of the price of the metal oxides (economic aspect), $AgNO_3$ was selected as an antimicrobial additive in further experiments.

3.2. PES−Chit−Ag_2O. *3.2.1. Pure Water Flux.* In this section, chitosan and $AgNO_3$ as additives were used simultaneously and further evaluated. The PWF of the membranes was measured (Figure 3). The addition of chitosan with the concentration ranging from 0.15 to 0.25% wt increased the PWF from 54.37 to 61.47 $L{\cdot}m^{-2}{\cdot}h^{-1}$. Furthermore, the addition of $AgNO_3$ increased the water flux from 58.66 to 68.46 $L{\cdot}m^{-2}{\cdot}h^{-1}$. This result indicates that the addition of chitosan and $AgNO_3$ exerted a synergetic effect on PWF. The PWF of the porous membrane is influenced by several factors, such as the pore size, porosity, pore structure, membrane thickness, and wettability. The modified chitosan and Ag_2O membrane has a greater pore size than the pure PES membrane, as observed in Section 3.2.5. However, this incorporation into PES membranes increased their hydrophilicity and PWF (see Section 3.2.6). The identical outcomes were reported by Al-Amoudi and Farooque.[50,51]

3.2.2. Adsorptive Fouling Performance. Figure 4 shows the results of RFR during adsorptive fouling evaluation. The occurrence of adsorptive fouling in UF PES membranes is not surprising, and the reasons for this phenomenon have been documented.[8,12,52] Aside from being affected by the physical membrane structure (including surface and pore structures), the hydrophobicity of the PES polymer has an impact on the occurrence of adsorptive fouling.

Addition of chitosan and $AgNO_3$ decreased the RFR, indicating that less adsorptive fouling occurred. Addition of chitosan (only) decreased the RFR from 46.66 to 44.25% under acidic conditions, whereas addition of $AgNO_3$ (only) decreased the RFR from 46.66 to 39.12%. Interestingly, addition of chitosan and $AgNO_3$ simultaneously decreased the RFR from 46.66 to 34.11%. Under alkaline conditions, a decreasing trend also occurred in the addition of chitosan (only) from 47.32 to 43.31% and the addition of $AgNO_3$ (only) from 47.32 to 36.54%, and the addition of both decreased from 47.32 to 36.54%. This result suggests that the combination of chitosan and $AgNO_3$ is an attractive additive to be used for manufacturing low-fouling PES UF membranes. Hydrophilic membranes have larger water bonding energy with a membrane surface than protein bonds with membrane surfaces.[53] As a result, less protein is adsorbed on the surface of the membrane.

The effect of additives on decreasing RFR after adsorption was observed under alkaline (pH 8) and acidic (pH 5) conditions. At both pH values, the modified membranes had lower RFR than the PES (only) membrane. This result suggests that the modification via hydrophilization by chitosan and Ag_2O was relevant for negative and neutral charge membranes. The higher RFR at pH 5 than that at pH 8 can be ascribed to the fact that the iso-electric point of BSA is approximately pH 4.8.[54,55] At this pH, the BSA has neutral pH, more hydrophobicity, and low solubility. As a result, the amount of BSA adsorbing on the membrane surface increases.

3.2.3. Cross-Flow Relative Flux. Cross-flow filtration was used to test the membrane's performance in a practical implementation. For all membranes tested, the permeate flux dropped considerably at the start of filtering (Figure 5).

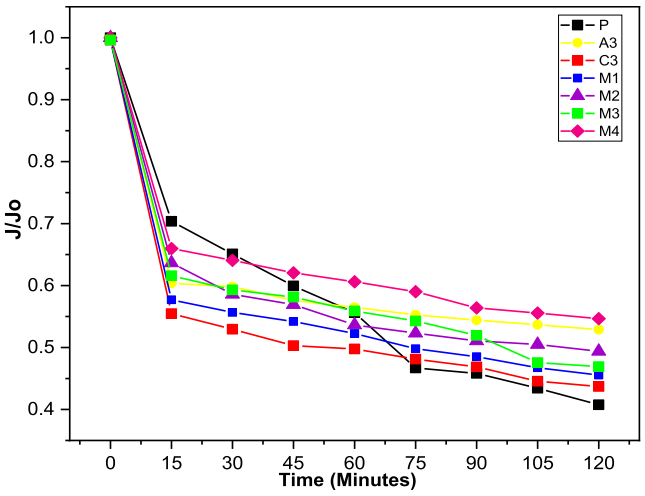

Figure 5. Cross-flow relative flux as a function of filtration time on the PES−chitosan−Ag_2O membranes.

Concentration polarization contributed to these fluxes declines, but fouling was also identified as a contributing factor in the flow reduction. It can alter fouling through membrane−solute and/or solute−solute interaction. The PES membrane (only) had the most fouling, as indicated by its lowest flux ratio even though it showed the highest flux ratio at the beginning of filtration. Incorporation of $AgNO_3$ and chitosan clearly increased the membrane fouling resistance, with the lowest fouling demonstrated by the M4 membrane. The influence of $AgNO_3$ and chitosan was clearly observed.

The flux ratio of the PES membrane (only) decreased to 0.407 at 120 min. The addition of chitosan (only) decreased the ratio up to 0.480, whereas the ratio decreased to 0.528 with the addition of $AgNO_3$ (only). The flux decline at the beginning of the filtration is mainly due to concentration polarization. The effect of flux reduction owing to concentration polarization is less noticeable the lower the porosity. At

https://doi.org/10.1021/acsomega.2c03685
ACS Omega 2022, 7, 46066−46078

the beginning of the filtration, where the flux decline is mainly caused by concentration polarization, the PES (only) membrane showed the lowest flux decline. The possible reason for this phenomenon is that the control PES membrane has the lowest porosity, as evidenced by its lowest PWF (Figures 1 and 3). The lower the porosity, the smaller the impact of flux reduction caused by concentration polarization.

The presence of chitosan and Ag_2O in the PES membrane increased the cleaning rate of proteins attached to the surface of the membrane faster than the fouling rate formation by proteins.[31] Thus, the modified membranes reduced fouling formation on the surface of the membrane and increased flux. Interestingly, the combination of chitosan and Ag_2O improved performance compared with chitosan or Ag_2O only. This result was evidenced by the greater reduction ratios of the M1 to M4 membranes than those of pure PES membranes, with the largest flux reduction ratio (0.540) owned by M4 membranes. Therefore, the modified membranes are more resistant to fouling than the other membranes.

3.2.4. Membrane Functional Groups. FTIR spectroscopy was used to investigate the chemistry of the membrane surface. The results are presented in Figure 6. The structure of PES is

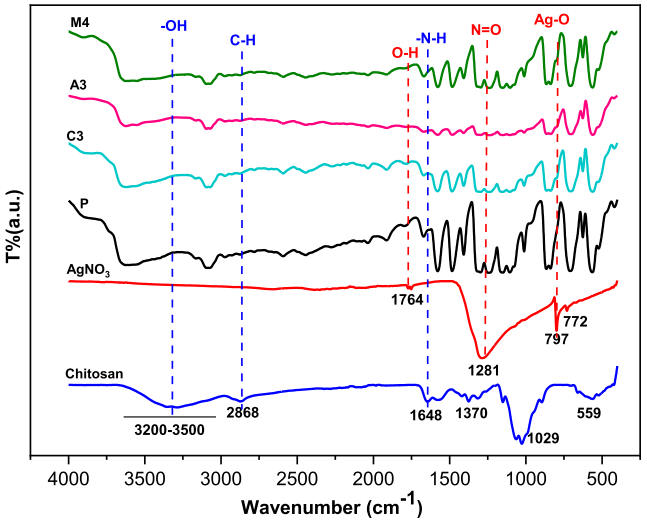

Figure 6. FTIR spectra of PES membranes.

devoid of O−H bonds. As a result, the O−H stretching of water molecules is allocated to the band around 3500−3700 cm^{-1}. The sulfone group (O═S═O stretching) is represented by the peaks at 1296.42 cm^{-1}, whereas the aromatic ether is represented by the peak at 1240.5 cm^{-1} (C−O−C stretching), 1483.14 cm^{-1} (C═C stretching), and 3095.57 cm^{-1} (C−H stretching). C−S stretching may be responsible for the peak at 706.33 cm^{-1}.[56]

On chitosan, peaks related to the −OH vibration were found at 3200−3600 cm^{-1}.[20,33] The peak at 1648 cm^{-1} corresponded to the −NH deformation vibration of chitosan (amide I band, amide II). Strain vibrations C−H of methylene and methyl chitosan were ascribed to other peaks at 2868.64 cm^{-1}. Baio et al. also detected this peak at 2885 cm^{-1};[57] on the PES−chitosan membrane, namely, the C3 and M4 membranes, peaks in the chitosan group were also formed. The membrane modification by addition of $AgNO_3$ resulting in the peak at 797 cm^{-1}[58] was formed due to the interaction of Ag−O groups and also in 1281 cm^{-1} in the form of −N═O groups.[59] This group is also formed on A3 and M4 membranes.

3.2.5. SEM Analysis. SEM images of PES (only) and PES-modified membranes with chitosan and $AgNO_3$ can be seen in Figure 7. All membranes have an asymmetric structure, displaying a finger-like pore structure, according to the cross-section structure. The addition of chitosan to the membrane resulted in a more porous membrane surface than that of pure PES membranes. The PES−Ag_2O membrane has a bigger and more uniform pore size than the PES−chitosan membrane. Overall, the SEM images support the previous water flux measurements.

Figure 7 shows SEM images of PES membranes (pure) and PES treated with chitosan and $AgNO_3$. The membrane pores are visible as black dots in contrast to other regions in SEM picture 7a, which depicts the surface morphology of each membrane. It is obvious that the PES (P) membrane has smaller pores than the C1 membrane that has received chitosan modification. Additionally, chitosan particles were seen on the C1 membrane's surface, while on the A2 and M4 membranes, Ag compounds are also visible as uniformly distributed white granules. Ag is totally dissolved when it is mixed into the PES membrane dope solution; there can be an even dispersion on the surface of this membrane with no agglomeration. On all modified membranes with pores bigger than those of the P membrane, water absorption or flux values increased, and CA values decreased, indicating that the membrane surface was more hydrophilic.

In the Figure 7b cross-sectional picture, it can be seen that all membranes have an asymmetrical structure and display a finger-like pore structure. The NIPS technique utilized to create the membrane is responsible for the membrane's asymmetrical pore shape. The created pores have varying diameters from top to bottom. Asymmetric membranes typically consist of three crucial components. The uppermost surface layer with the lowest pore size is known as the active layer or top layer. This active layer functions as the first part that comes into contact with water or pollutants; this part is what determines whether the compound can pass through the membrane or not. The membrane's secondary filtering is carried out by the second component, which is referred to as the secondary pore and includes a small pore. The second part is called the secondary pore which consists of a narrow pore for secondary filtration on the membrane. Pollutants that pass the filtration stage in the active layer may be retained in this secondary pore. If the pollutant is retained, irreversible fouling can occur on the membrane. The third part is the bottom layer which consists of a wide pore that functions as a part that maintains membrane stability during filtration. The addition of chitosan to the membrane resulted in a more porous membrane surface than that of pure PES membranes. PES−Ag_2O had larger and uniform pore sizes than PES−chitosan membranes. Overall, the SEM images support the previous water flux measurements.

3.2.6. Hydrophilicity. Membrane wettability was investigated by CA measurements. The CA of PES and chitosan films (prepared by spin-coating) was also included. The results are represented in Figure 8. The PES film and PES membrane (only) showed a CA of 79.50 ± 1.2 and 73.22 ± 1°, respectively. This value may be different from the results reported in previous publications (e.g., ref 8). The difference in pore size and porosity is believed to be the main reason for this condition. The difference in the CA between the PES film

https://doi.org/10.1021/acsomega.2c03685
ACS Omega 2022, 7, 46066−46078

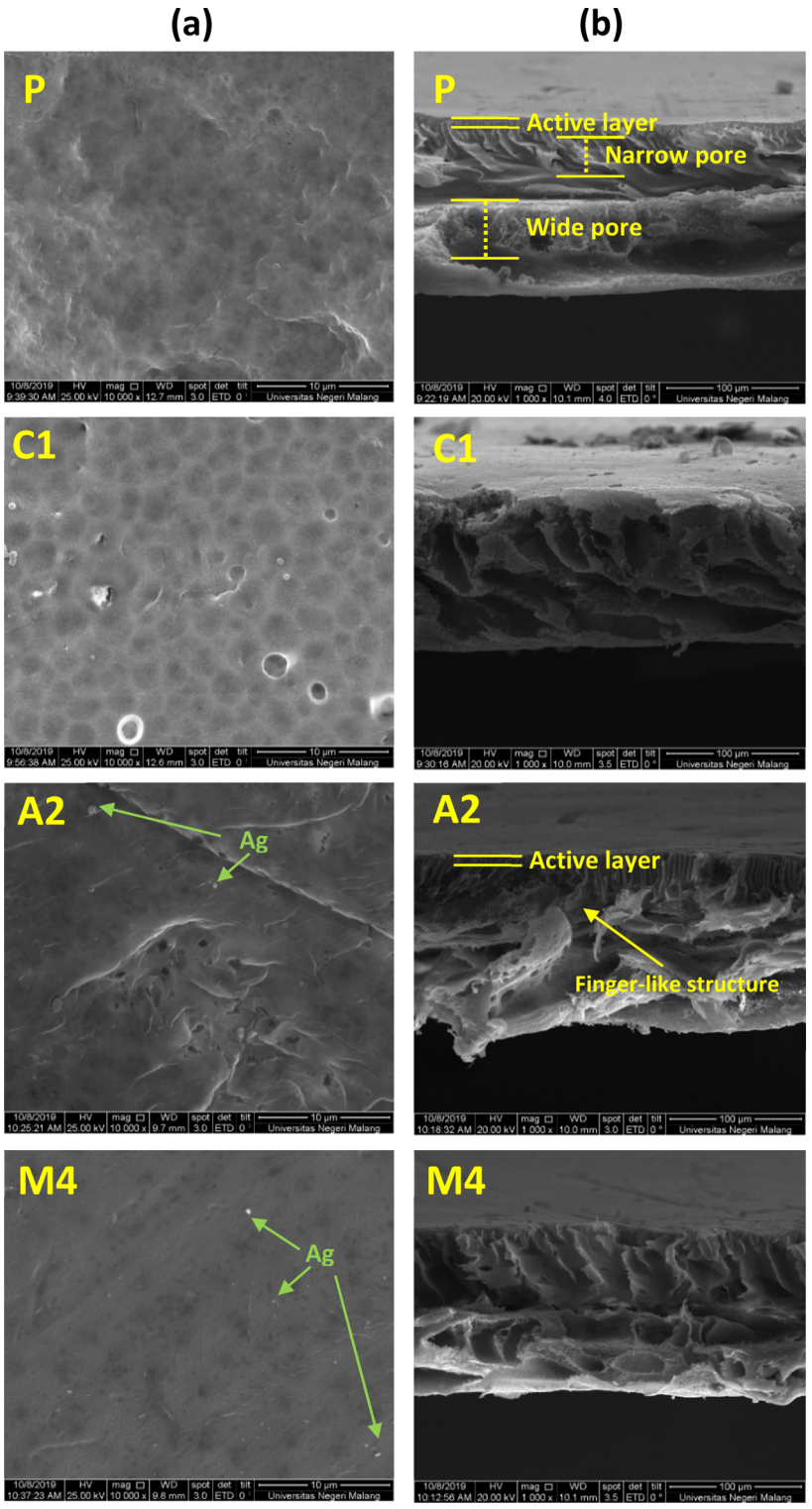

Figure 7. Scanning electron microscope image: (a) cross-section with magnification 1000× and (b) membrane surface magnification 10,000×.

(non-porous) and PES membrane (porous) supports this explanation. The addition of chitosan (only), $AgNO_3$ (only), and chitosan−$AgNO_3$ together into the PES membrane decreased the membrane CA. The addition of chitosan (only) into the PES membrane decreased the CA from 73.22 to 55.82°, proving that hydrophilization occurred after chitosan addition. However, increasing membrane porosity is believed to be the reason for the increase in membrane hydrophilicity (by decreasing the CA). Note that the CA of the chitosan film was higher than the CA of the PES film (82.33 vs 79.5°). The hydrophobic backbone of chitosan caused its CA to become unusually high, displaying hydrophobic character, despite the fact that chitosan is a hydrophilic biopolymer that should have low CA indicating its hydrophilic character.[60] These conditions suggest that the decrease in the CA after the addition of chitosan is caused by the increase in porosity. It seems that chitosan can act as a pore forming agent. Identical outcomes were observed when 2% wt $AgNO_3$ was poured into

https://doi.org/10.1021/acsomega.2c03685
ACS Omega 2022, 7, 46066−46078

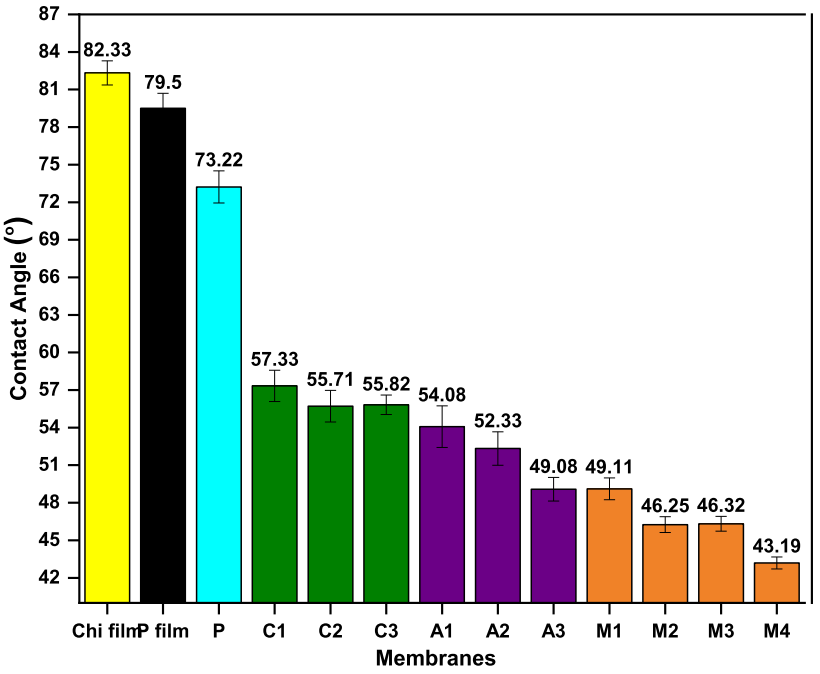

Figure 8. CA (°) of different membranes.

the PES membrane where the CA decreased to 49.08°. The incorporation of these two compounds in the PES membrane provides a synergistic effect as evidenced by a better reduction in the CA value compared with the mixing carried out separately, as evidenced by the M4 membrane type, which has a CA value of 43.19°. In general, the membrane flux is influenced by many variables such as membrane porosity and membrane hydrophilicity. The increases in membrane porosity and membrane hydrophilicity increase the membrane flux. The increase in hydrophilicity increases the water penetration into the membrane causing an increase in flux. Nevertheless, it is important to note that the value of the water CA is also influenced by the membrane porosity, where the increase in porosity decreases the membrane CA or increases membrane hydrophilicity.

3.2.7. Antibacterial Activities. In this work, the antibacterial ability was observed by the ZoI method. The results are presented in Figure 9. The PES (only) membrane showed no ZoI for *E. coli* and *S. aureus*. Modification of the PES−chitosan membrane with 0.25% wt chitosan shows a few antibacterial agents. This is attributed to chitosan's ineffective antibacterial action in acidic environments.[61] The modified PES−Ag_2O membrane with a concentration of $AgNO_3$ of 1, 1.5, and 2% wt showed a slight ZoI. The formation of the ZoI was more significant when $AgNO_3$ and chitosan were used simultaneously for PES modification than when they were used alone. Thus, the compositions of chitosan and $AgNO_3$ was investigated to maximize the antimicrobial activity. The chitosan concentration was 0.25% wt, whereas the $AgNO_3$ concentration was varied from 0.5 to 2% wt.

The combination of chitosan−$AgNO_3$ demonstrated a greater bactericidal efficiency than chitosan or $AgNO_3$ alone (Figure 9). The antibacterial ability of the chitosan−Ag_2O-modified PES membrane was better against *E. coli* than that against *S. aureus*. The higher the content of Ag_2O in the membrane, the greater the ZoI was formed. The value of the formed ZoI area can be seen in Table 2. The antibacterial

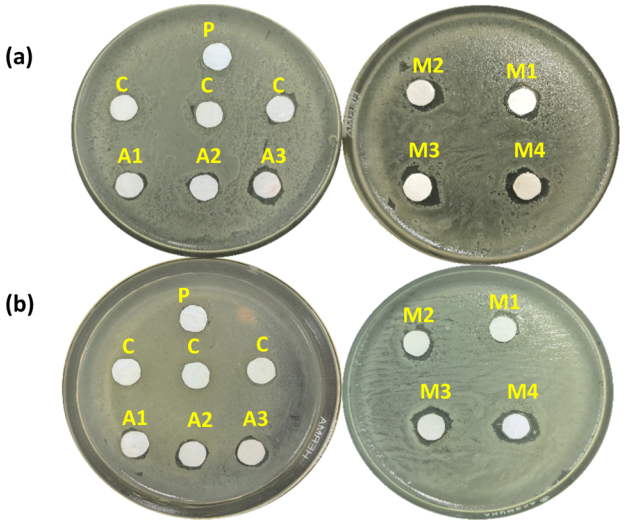

Figure 9. ZoI test for (a) *E. coli* and (b) *S. aureus* on the PES−chitosan−Ag_2O membrane.

Table 2. ZoI Area from the Antibacterial Test of *E. coli* and *S. aureus*

	ZoI area (mm^2)	
membrane	*E. coli*	*S. aureus*
P	1.409	2.816
C1	12.089	8.226
C2	19.900	9.556
C3	25.923	8.225
A1	23.359	13.689
A2	27.385	28.097
A3	41.349	25.965
M1	53.736	30.289
M2	56.316	39.291
M3	70.115	48.466
M4	87.518	72.963

https://doi.org/10.1021/acsomega.2c03685
ACS Omega 2022, 7, 46066−46078

activity of Ag_2O is related to its small size and high surface-to-volume ratio, which enables it to engage closely with microbial membranes rather than discharging metal ions toward solution.[57]

The antibacterial property of chitosan−Ag_2O can be attributed to Ag_2O's degradation of cell membranes coupled with the release of the silver cation on the membrane.[62] The interaction of silver with the cysteine−thiol group is thought to be the antibacterial mechanism.[63] Silver ions can combine with thiol groups to generate S−Ag complexes, which impede the afflicted proteases' normal enzymatic action. The released active silver cations attach onto the surface of the bacterial cell membrane through endocytosis.[57] The combination of chitosan and $AgNO_3$ produces an agent with strong antibacterial activity.

3.2.8. Membrane Surface Charge Analysis. The surface charge of the membrane was observed by measuring the zeta potential. The results are presented in Figure 10. It is seen that

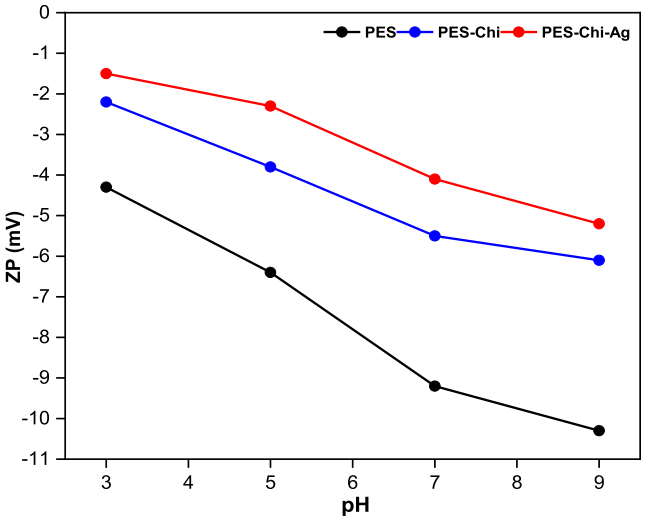

Figure 10. Zeta potential of different membranes.

all membranes demonstrated a negative surface charge over the entire pH range observed. The addition of chitosan changed the membrane surface charge toward being less negative. The negative charge of the membrane surface was further decreased by addition of silver nitrate into polymer membrane solution. The presence of the protonated amine group ($-NH_3^+$) from chitosan and silver decreases the negative charge of the PES membrane. Overall, the addition of chitosan and silver nitrate into PES solution produced membranes having lower negative charge compared to that of the PES (only) membrane. This will contribute to the lower electrostatic interaction of the membrane with the components in feed. Note that the BSA solution used (pH = 5) should have slightly negative charge. However, this charge interaction did not influence significantly the resulting organic fouling.

3.2.9. Membrane Stability Analysis. The modification stability was examined by immersing the membrane in distilled water for 21 days (membranes A3 and M4). The dripping water was analyzed with XRF every 3 days. The results are presented in Figure 11 and Table 3. It is seen that there was a small portion of Ag released into the water, that is, 1.719×10^{-5} g/L for A3 and 1.563×10^{-5} g/L for M4. Overall, the leakage is less than 1% after 21 days of immersion.

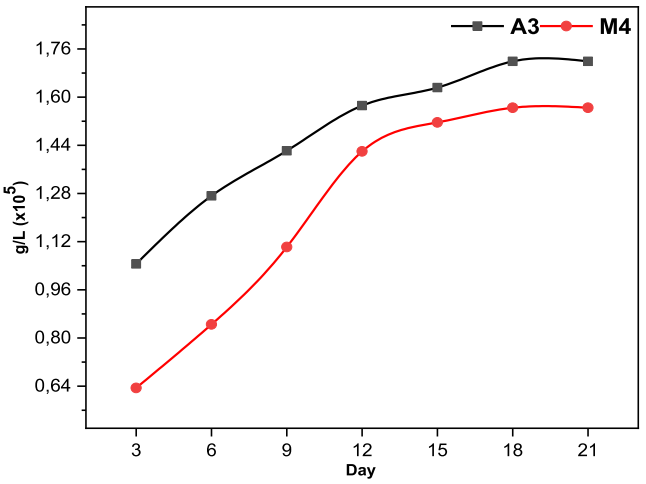

Figure 11. Ag release in water for the membrane stability test in 21 days.

Table 3. XRF Data Composition of Membranes

compound	XRF recorded	result (mass %) A3	result (mass %) M4
	Element		
silicone	Si	0.2200	0.1780
potassium	K	0.0344	0.0330
calcium	Ca	0.0087	0.0108
silver	Ag	0.0021	0.0018
	Oxide		
silicon dioxide	SiO_2	0.4710	0.3810
potassium oxide	K_2O	0.0415	0.0395
calcium oxide	CaO	0.0122	0.0157
silver oxide	Ag_2O	0.0023	0.0018

Interestingly, the release of Ag was smaller for the membrane containing chitosan. This observation may be caused by the interaction between Ag and chitosan.

Figure 11 shows the release of silver oxide during stability investigation. The silver compound released into the water was detected as silver oxide. This XRF test suggests that $AgNO_3$ added to the membrane dope solution was converted into Ag^+ ions and then reduced to Ag_2O during the NIPS process. This reduction process was indicated by the change in the color of dope solution from clear color to brownish yellow.[64] The amount of Ag_2O released from the A3 membrane was 0.0023% and from the M4 membrane was 0.0018%. Overall, the stability test demonstrated that the leakage of silver oxide from the membrane occurs, but the remaining silver oxide in the membrane was still much more significant.

To investigate the performance of the membrane that has been immersed for 21 days, the bacterial ZoI was analyzed. The results are presented in Figure 12. The antibacterial test demonstrated that the membrane that has been immersed for 21 days still had good antibacterial properties against *E. coli* and *S. aureus* bacteria as indicated by the formation of the ZoI area. However, the ZoI area formed was smaller compared to that of the pristine M4 membrane. The ZoI area for the M4 pristine membrane was 82.562 mm^2 and for M4 (immersed) was 67.291 mm^2 for *E. coli* bacteria. A similar phenomenon was observed for *S. aureus*.

The chitosan stability in the membrane was also investigated. FTIR was used to confirm the presence of

https://doi.org/10.1021/acsomega.2c03685
ACS Omega 2022, 7, 46066−46078

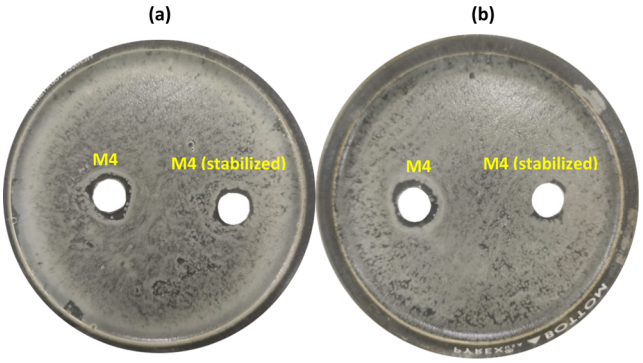

Figure 12. ZoI test for (a) *E. coli* and (b) *S. aureus* on M4 and M4 (stabilized).

chitosan in the membrane. The results are presented in Figure 13. The typical functional groups of chitosan in the membrane

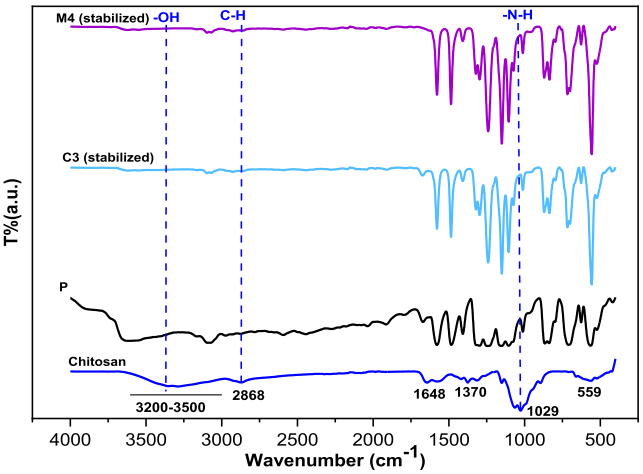

Figure 13. FTIR spectra of PES−chitosan membranes after the stability test.

(the −OH vibration peaks found at 3200−3600 and 1648 cm^{-1} correspond to −NH and also vibration CH peaks at 2868.64 cm^{-1}) could still be observed after soaking for 21 days.

4. CONCLUSIONS

The PES membrane was modified using chitosan and metal oxides to increase organic and biofouling resistance. Among several metal oxides that were evaluated, $AgNO_3$ showed the best performance. The addition of metal oxides increased the PWF of the modified membrane and reduced fouling on the membrane. The PES membrane with 0.25% wt chitosan and 2.0% wt $AgNO_3$ had the highest flux and highest antibacterial activity. The PWF increased with the addition of chitosan and $AgNO_3$. The effects of Ag and chitosan on the membrane structure, such as the CA, were investigated. The CA of the membranes decreased with chitosan and Ag loading. The PES−chitosan 0.25% wt−Ag_2O (from $AgNO_3$ 2.0% wt) (M4) membrane exhibited high antibacterial activity against *E. coli* and *S. aureus* bacteria, whereas the PES−Ag_2O membrane did not show the same result. In conclusion, the incorporation of chitosan into the PES−Ag_2O membrane increased its antibacterial activity substantially.

AUTHOR INFORMATION

Corresponding Author

Heru Susanto − *Department of Chemical Engineering, Faculty of Engineering, Diponegoro University, Tembalang-Semarang 50275, Indonesia; Membrane Research Center (Mer-C), PUI Membrane Central Laboratory for Research and Service, Diponegoro University, Semarang 50275, Indonesia;* orcid.org/0000-0002-0258-7437; Phone: (62)-24-7460058; Email: heru.susanto@che.undip.ac.id; Fax: (62)-24-76480675

Authors

Herlambang Abriyanto − *Department of Chemical Engineering, Faculty of Engineering, Diponegoro University, Tembalang-Semarang 50275, Indonesia; Membrane Research Center (Mer-C), PUI Membrane Central Laboratory for Research and Service, Diponegoro University, Semarang 50275, Indonesia*

Talita Maharani − *Department of Chemical Engineering, Faculty of Engineering, Diponegoro University, Tembalang-Semarang 50275, Indonesia*

Abdullah M. I. Filardli − *Department of Chemical Engineering, Faculty of Engineering, Diponegoro University, Tembalang-Semarang 50275, Indonesia; Membrane Research Center (Mer-C), PUI Membrane Central Laboratory for Research and Service, Diponegoro University, Semarang 50275, Indonesia*

Ria Desiriani − *Department of Chemical Engineering, Faculty of Engineering, Diponegoro University, Tembalang-Semarang 50275, Indonesia; Membrane Research Center (Mer-C), PUI Membrane Central Laboratory for Research and Service, Diponegoro University, Semarang 50275, Indonesia*

Nita Aryanti − *Department of Chemical Engineering, Faculty of Engineering, Diponegoro University, Tembalang-Semarang 50275, Indonesia; Membrane Research Center (Mer-C), PUI Membrane Central Laboratory for Research and Service, Diponegoro University, Semarang 50275, Indonesia*

Complete contact information is available at: https://pubs.acs.org/10.1021/acsomega.2c03685

Author Contributions

CRediT authorship contribution statement: H.S.: conceptualization, methodology, resources, and writing-review and editing. H.A. and T.M.: methodology, investigation, data caution, and writing-original draft. N.A.: validation, data curation, and formal analysis. A.I.F.M. and R.D.: editing and formal analysis.

Notes

The authors declare no competing financial interest.

ACKNOWLEDGMENTS

The authors would like to thank Diponegoro University for the research funding through the Pendidikan Magister Menuju Doktor Untuk Sarjana Unggul Universitas Diponegoro (PMDSU-UNDIP), grant number 14-01/UN7.P4.3/PP/2020. The authors would also like to thank the Department of Chemical Engineering, Faculty of Engineering, Diponegoro University, Integrated Laboratory Diponegoro University, and the Membrane Research Center (Mer-C) for the supporting facilities while conducting this project.

https://doi.org/10.1021/acsomega.2c03685
ACS Omega 2022, 7, 46066−46078

REFERENCES

(1) Huang, J.; Zhang, K.; Wang, K.; Xie, Z.; Ladewig, B.; Wang, H. Fabrication of Polyethersulfone-Mesoporous Silica Nanocomposite Ultrafiltration Membranes with Antifouling Properties. *J. Membr. Sci.* **2012**, *423*−*424*, 362−370.

(2) Farjami, M.; Vatanpour, V.; Moghadassi, A. Effect of Nanoboehmite/Poly(Ethylene Glycol) on the Performance and Physiochemical Attributes EPVC Nano-Composite Membranes in Protein Separation. *Chem. Eng. Res. Des.* **2020**, *156*, 371−383.

(3) Kochkodan, V.; Hilal, N. A Comprehensive Review on Surface Modified Polymer Membranes for Biofouling Mitigation. *Desalination* **2015**, *356*, 187−207.

(4) Zhao, S.; Yan, W.; Shi, M.; Wang, Z.; Wang, J.; Wang, S. Improving Permeability and Antifouling Performance of Polyethersulfone Ultrafiltration Membrane by Incorporation of ZnO-DMF Dispersion Containing Nano-ZnO and Polyvinylpyrrolidone. *J. Membr. Sci.* **2015**, *478*, 105−116.

(5) Saxena, A.; Tripathi, B. P.; Kumar, M.; Shahi, V. K. Membrane-Based Techniques for the Separation and Purification of Proteins: An Overview. *Adv. Colloid Interface Sci.* **2009**, *145*, 1−22.

(6) Huang, H.; Yu, J.; Guo, H.; Shen, Y.; Yang, F.; Wang, H.; Liu, R.; Liu, Y. Improved Antifouling Performance of Ultrafiltration Membrane via Preparing Novel Zwitterionic Polyimide. *Appl. Surf. Sci.* **2018**, *427*, 38−47.

(7) Biswas, P.; Bandyopadhyaya, R. Biofouling Prevention Using Silver Nanoparticle Impregnated Polyethersulfone (PES) Membrane: E. Coli Cell-Killing in a Continuous Cross-Flow Membrane Module. *J. Colloid Interface Sci.* **2017**, *491*, 13−26.

(8) Huang, J.; Wang, H.; Zhang, K. Modification of PES Membrane with Ag-SiO2: Reduction of Biofouling and Improvement of Filtration Performance. *Desalination* **2014**, *336*, 8−17.

(9) Gul, S.; Rehan, Z. A.; Khan, S. A.; Akhtar, K.; Khan, M. A.; Khan, M. I.; Rashid, M. I.; Asiri, A. M.; Khan, S. B. Antibacterial PES-CA-Ag2O Nanocomposite Supported Cu Nanoparticles Membrane toward Ultrafiltration, BSA Rejection and Reduction of Nitrophenol. *J. Mol. Liq.* **2017**, *230*, 616−624.

(10) Mu, Y.; Zhu, K.; Luan, J.; Zhang, S.; Zhang, C.; Na, R.; Yang, Y.; Zhang, X.; Wang, G. Fabrication of Hybrid Ultrafiltration Membranes with Improved Water Separation Properties by Incorporating Environmentally Friendly Taurine Modified Hydroxyapatite Nanotubes. *J. Membr. Sci.* **2019**, *577*, 274−284.

(11) Susanto, H.; Robbani, M. H.; Istirokhatun, T.; Firmansyah, A. A.; Rhamadhan, R. N. Preparation of Low-Fouling Polyethersulfone Ultrafiltration Membranes by Incorporating High-Molecular-Weight Chitosan with the Help of a Surfactant. *S. Afr. J. Chem. Eng.* **2020**, *33*, 133−140.

(12) Samari, M.; Zinadini, S.; Zinatizadeh, A. A.; Jafarzadeh, M.; Gholami, F. Designing of a Novel Polyethersulfone (PES) Ultrafiltration (UF) Membrane with Thermal Stability and High Fouling Resistance Using Melamine-Modified Zirconium-Based Metal-Organic Framework (UiO-66-NH2/MOF). *Sep. Purif. Technol.* **2020**, *251*, 117010.

(13) Susanto, H.; Ulbricht, M.Polymeric Membranes for Molecular Separations. *Membrane Operations: Innovative Separations and Transformations*; Wiley, 2009; 19−43.

(14) Ayyavoo, J.; Nguyen, T. P. N.; Jun, B. M.; Kim, I. C.; Kwon, Y. N. Protection of polymeric membranes with antifouling surfacing via surface modifications. *Colloids Surf., A* **2016**, *506*, 190−201.

(15) Zhu, L. J.; Zhu, L. P.; Zhao, Y. F.; Zhu, B. K.; Xu, Y. Y. Antifouling and anti-bacterial polyethersulfone membranes quaternized from the additive of poly(2-dimethylamino ethyl methacrylate) grafted SiO2nanoparticles. *J. Mater. Chem. A* **2014**, *2*, 15566−15574.

(16) Zodrow, K.; Brunet, L.; Mahendra, S.; Li, D.; Zhang, A.; Li, Q.; Alvarez, P. J. J. Polysulfone Ultrafiltration Membranes Impregnated with Silver Nanoparticles Show Improved Biofouling Resistance and Virus Removal. *Water Res.* **2009**, *43*, 715−723.

(17) Baker, J. S.; Dudley, L. Y. Biofouling in Membrane Systems—a Review. *Desalination* **1998**, *118*, 81−89.

(18) Watanabe, N.; Suga, K.; Umakoshi, H. Functional Hydration Behavior: Interrelation between Hydration and Molecular Properties at Lipid Membrane Interfaces. *J. Chem.* **2019**, *2019*, 4867327.

(19) Kandori, K.; Oketani, M.; Wakamura, M. Effects of Ti(IV) Substitution on Protein Adsorption Behaviors of Calcium Hydroxyapatite Particles. *Colloids Surf., B* **2013**, *101*, 68−73.

(20) Boributh, S.; Chanachai, A.; Jiraratananon, R. Modification of PVDF Membrane by Chitosan Solution for Reducing Protein Fouling. *J. Membr. Sci.* **2009**, *342*, 97−104.

(21) Susanto, H.; Malik, A. I. F.; Raharjo, S. H.; Nur, M. Preparation and Characterization of High Flux Polypropylene Microfiltration Membrane via Non-Solvent Induced Phase Separation. *Mater. Today: Proc.* **2019**, *13*, 276−280.

(22) Elizalde, C. N. B.; Al-Gharabli, S.; Kujawa, J.; Mavukkandy, M.; Hasan, S. W.; Arafat, H. A. Fabrication of Blend Polyvinylidene Fluoride/Chitosan Membranes for Enhanced Flux and Fouling Resistance. *Sep. Purif. Technol.* **2018**, *190*, 68−76.

(23) Bagheripour, E.; Moghadassi, A. R.; Parvizian, F.; Hosseini, S. M.; Van der Bruggen, B. Tailoring the Separation Performance and Fouling Reduction of PES Based Nanofiltration Membrane by Using a PVA/Fe3O4 Coating Layer. *Chem. Eng. Res. Des.* **2019**, *144*, 418−428.

(24) Matabola, K. P.; Bambo, M. F.; Sikhwivhilu, K.; Vatsha, B.; Moutloali, R. M. Chemical Grafting of Polystyrene Sodium Sulfonate (PSS) onto Polyethersulfone (PES) Powder and Effect on the Characteristics of the Resultant Ultrafiltration Membranes. *Mater. Today: Proc.* **2015**, *2*, 3957−3963.

(25) Daraei, P.; Madaeni, S. S.; Ghaemi, N.; Ahmadi Monfared, H.; Khadivi, M. A. Fabrication of PES Nanofiltration Membrane by Simultaneous Use of Multi-Walled Carbon Nanotube and Surface Graft Polymerization Method: Comparison of MWCNT and PAA Modified MWCNT. *Sep. Purif. Technol.* **2013**, *104*, 32−44.

(26) Li, Q.; Bi, Q.-y.; Lin, H.-H.; Bian, L.-X.; Wang, X.-L. A Novel Ultrafiltration (UF) Membrane with Controllable Selectivity for Protein Separation. *J. Membr. Sci.* **2013**, *427*, 155−167.

(27) Susanto, H.; Ulbricht, M. Characteristics, Performance and Stability of Polyethersulfone Ultrafiltration Membranes Prepared by Phase Separation Method Using Different Macromolecular Additives. *J. Membr. Sci.* **2009**, *327*, 125−135.

(28) Zhao, Y. H.; Qian, Y. L.; Zhu, B. K.; Xu, Y. Y. Modification of Porous Poly(Vinylidene Fluoride) Membrane Using Amphiphilic Polymers with Different Structures in Phase Inversion Process. *J. Membr. Sci.* **2008**, *310*, 567−576.

(29) Azhar, O.; Jahan, Z.; Sher, F.; Niazi, M. B. K.; Kakar, S. J.; Shahid, M. Cellulose Acetate-Polyvinyl Alcohol Blend Hemodialysis Membranes Integrated with Dialysis Performance and High Biocompatibility. *Mater. Sci. Eng. C* **2021**, *126*, 112127.

(30) Silva, L. L. S.; Abdelraheem, W.; Nadagouda, M. N.; Rocco, A. M.; Dionysiou, D. D.; Fonseca, F. V.; Borges, C. P. Novel Microwave-Driven Synthesis of Hydrophilic Polyvinylidene Fluoride/Polyacrylic Acid (PVDF/PAA) Membranes and Decoration with Nano Zero-Valent-Iron (NZVI) for Water Treatment Applications. *J. Membr. Sci.* **2021**, *620*, 118817.

(31) Xiong, S.; Han, C.; Phommachanh, A.; Li, W.; Xu, S.; Wang, Y. High-Performance Loose Nanofiltration Membrane Prepared with Assembly of Covalently Cross-Linked Polyethyleneimine-Based Polyelectrolytes for Textile Wastewater Treatment. *Sep. Purif. Technol.* **2021**, *274*, 119105.

(32) Shi, H.; Xue, L.; Gao, A.; Fu, Y.; Zhou, Q.; Zhu, L. Fouling-Resistant and Adhesion-Resistant Surface Modification of Dual Layer PVDF Hollow Fiber Membrane by Dopamine and Quaternary Polyethyleneimine. *J. Membr. Sci.* **2016**, *498*, 39−47.

(33) Kumar, R.; Isloor, A. M.; Ismail, A. F.; Rashid, S. A.; Matsuura, T. Polysulfone-Chitosan Blend Ultrafiltration Membranes: Preparation, Characterization, Permeation and Antifouling Properties. *RSC Adv.* **2013**, *3*, 7855−7861.

(34) Ma, Y.; Zhou, T.; Zhao, C. Preparation of Chitosan-Nylon-6 Blended Membranes Containing Silver Ions as Antibacterial Materials. *Carbohydr. Res.* **2008**, *343*, 230−237.

https://doi.org/10.1021/acsomega.2c03685
ACS Omega 2022, 7, 46066−46078

(35) Istirokhat, T.; Rokhati, N.; Nurlaeli, D.; Arifianing, N. N.; Sudarno; Syafrudin; Susanto, H. Characteristics, Biofouling Properties and Filtration Performance of Cellulose/Chitosan Membranes. *J. Environ. Sci. Technol.* **2017**, *10*, 56−67.
(36) Chede, S.; Anaya, N. M.; Oyanedel-Craver, V.; Gorgannejad, S.; Harris, T. A. L.; Al-Mallahi, J.; Abu-Dalo, M.; Qdais, H. A.; Escobar, I. C. Desalination Using Low Biofouling Nanocomposite Membranes: From Batch-Scale to Continuous-Scale Membrane Fabrication. *Desalination* **2019**, *451*, 81−91.
(37) Flemming, H.; Schaule, G.; Griebe, T.; Schmitt, J.; Tamachkiarowa, A. Biofouling-the Achilles heel of membrane processes. *Desalination* **1997**, *113*, 215−225.
(38) Shaheen, A.; Sultana, S.; Lu, H.; Ahmad, M.; Asma, M.; Mahmood, T. Assessing the potential of different nano-composite (MgO, Al 2 O 3 -CaO and TiO 2) for efficient conversion of Silybum eburneum seed oil to liquid biodiesel. *J. Mol. Liq.* **2018**, *249*, 511−521.
(39) Ma, G.; Xu, X.; Tesfai, M.; Wang, H.; Xu, P. Developing Anti-Biofouling and Energy-Efficient Cation-Exchange Membranes Using Conductive Polymers and Nanomaterials. *J. Membr. Sci.* **2020**, *603*, 118034.
(40) Yu, Y.; Yang, Y.; Yu, L.; Koh, K. Y.; Chen, J. P. Modification of Polyvinylidene Fluoride Membrane by Silver Nanoparticles-Graphene Oxide Hybrid Nanosheet for Effective Membrane Biofouling Mitigation. *Chemosphere* **2021**, *268*, 129187.
(41) Huang, J.; Wang, H.; Zhang, K. Modification of PES membrane with Ag-SiO2: Reduction of biofouling and improvement of filtration performance. *Desalination* **2014**, *336*, 8−17.
(42) Soleymani Lashkenari, A.; Hamed Mosavian, M. T.; Peyravi, M.; Jahanshahi, M. Biofouling Mitigation of Bilayer Polysulfone Membrane Assisted by Zinc Oxide-Polyrhodanine Couple Nanoparticle. *Prog. Org. Coat.* **2019**, *129*, 147−158.
(43) Ahsani, M.; Hazrati, H.; Javadi, M.; Ulbricht, M.; Yegani, R. Preparation of Antibiofouling Nanocomposite PVDF/Ag-SiO2 Membrane and Long-Term Performance Evaluation in the MBR System Fed by Real Pharmaceutical Wastewater. *Sep. Purif. Technol.* **2020**, *249*, 116938.
(44) Susanto, H.; Ulbricht, M. Influence of Ultrafiltration Membrane Characteristics on Adsorptive Fouling with Dextrans. *J. Membr. Sci.* **2005**, *266*, 132−142.
(45) Otitoju, T. A.; Ahmad, A. L.; Ooi, B. S. Polyethersulfone Composite Hollow-Fiber Membrane Prepared by in-Situ Growth of Silica with Highly Improved Oily Wastewater Separation Performance. *J. Polym. Res.* **2017**, *24*, 123.
(46) Shannon, M. A.; Bohn, P. W.; Elimelech, M.; Georgiadis, J. G.; Mariñas, B. J.; Mayes, A. M. Science and Technology for Water Purification in the Coming Decades. *Nature* **2008**, *452*, 301−310.
(47) Kanmani, P.; Rhim, J. W. Properties and Characterization of Bionanocomposite Films Prepared with Various Biopolymers and ZnO Nanoparticles. *Carbohydr. Polym.* **2014**, *106*, 190−199.
(48) Mao, Y.; Li, Y.; Zou, Y.; Shen, X.; Zhu, L.; Liao, G. Solvothermal Synthesis and Photocatalytic Properties of ZnO Micro/Nanostructures. *Ceram. Int.* **2019**, *45*, 1724−1729.
(49) Firouzjaei, M. D.; Seyedpour, S. F.; Aktij, S. A.; Giagnorio, M.; Bazrafshan, N.; Mollahosseini, A.; Samadi, F.; Ahmadalipour, S.; Firouzjaei, F. D.; Esfahani, M. R.; Tiraferri, A.; Elliott, M.; Sangermano, M.; Abdelrasoul, A.; McCutcheon, J. R.; Sadrzadeh, M.; Esfahani, A. R.; Rahimpour, A. Recent Advances in Functionalized Polymer Membranes for Biofouling Control and Mitigation in Forward Osmosis. *J. Membr. Sci.* **2020**, *596*, 117604.
(50) Shah, N.; Mewada, R. K.; Mehta, T. Chitosan: Development of Nanoparticles, Other Physical Forms and Solubility with Acids. *J. Nano Res.* **2013**, *24*, 107−122.
(51) Al-Amoudi, A. S.; Farooque, A. M. Performance Restoration and Autopsy of NF Membranes Used in Seawater Pretreatment. *Desalination* **2005**, *178*, 261−271.
(52) Basri, H.; Ismail, A. F.; Aziz, M. Polyethersulfone (PES)-Silver Composite UF Membrane: Effect of Silver Loading and PVP Molecular Weight on Membrane Morphology and Antibacterial Activity. *Desalination* **2011**, *273*, 72−80.
(53) Daraei, P.; Madaeni, S. S.; Ghaemi, N.; Khadivi, M. A.; Astinchap, B.; Moradian, R. Enhancing Antifouling Capability of PES Membrane via Mixing with Various Types of Polymer Modified Multi-Walled Carbon Nanotube. *J. Membr. Sci.* **2013**, *444*, 184−191.
(54) Yang, Q.; Liu, Y.; Li, Y. Control of Protein (BSA) Fouling in RO System by Antiscalants. *J. Membr. Sci.* **2010**, *364*, 372−379.
(55) Mo, H.; Tay, K. G.; Ng, H. Y. Fouling of Reverse Osmosis Membrane by Protein (BSA): Effects of PH, Calcium, Magnesium, Ionic Strength and Temperature. *J. Membr. Sci.* **2008**, *315*, 28−35.
(56) Ghiggi, F. F.; Pollo, L. D.; Cardozo, N. S. M.; Tessaro, I. C. Preparation and Characterization of Polyethersulfone/N-Phthaloyl-Chitosan Ultrafiltration Membrane with Antifouling Property. *Eur. Polym. J.* **2017**, *92*, 61−70.
(57) Biao, L.; Tan, S.; Wang, Y.; Guo, X.; Fu, Y.; Xu, F.; Zu, Y.; Liu, Z. Synthesis, Characterization and Antibacterial Study on the Chitosan-Functionalized Ag Nanoparticles. *Mater. Sci. Eng. C* **2017**, *76*, 73−80.
(58) Istirokhatun, T.; Lin, Y.; Shen, Q.; Guan, K.; Wang, S.; Matsuyama, H. Ag-Based Nanocapsule-Regulated Interfacial Polymerization Enables Synchronous Nanostructure towards High-Performance Nanofiltration Membrane for Sustainable Water Remediation. *J. Membr. Sci.* **2022120196**, *645*, 120196.
(59) Liu, H.; Bai, J.; Wang, S.; Li, C.; Guo, L.; Liang, H.; Xu, T.; Sun, W.; Li, H. The Preparation of Silver Nanoparticles/Carbon Nanofibers as Catalyst in the Styrene Epoxidation. *Colloids Surf., A* **2014**, *448*, 154−159.
(60) Almeida, E. V. R.; Frollini, E.; Castellan, A.; Coma, V. Chitosan, sisal cellulose, and biocomposite chitosan/sisal cellulose films prepared from thiourea/NaOH aqueous solution. *Carbohydr. Polym.* **2010**, *80*, 655−664.
(61) Helander, I. M.; Nurmiaho-Lassila, E. L.; Ahvenainen, R.; Rhoades, J.; Roller, S. Chitosan Disrupts the Barrier Properties of the Outer Membrane of Gram-Negative Bacteria. *Int. J. Food Microbiol.* **2001**, *71*, 235−244.
(62) Liu, C. X.; Zhang, D. R.; He, Y.; Zhao, X. S.; Bai, R. Modification of Membrane Surface for Anti-Biofouling Performance: Effect of Anti-Adhesion and Anti-Bacteria Approaches. *J. Membr. Sci.* **2010**, *346*, 121−130.
(63) Bashambu, L.; Singh, R.; Verma, J. Metal/Metal Oxide Nanocomposite Membranes for Water Purification. *Mater. Today: Proc.* **2021**, *44*, 538−545.
(64) Arif, M. S.; Ulfiya, R.; Erwin; Panggabean, A. S. Synthesis Silver Nanoparticles Using Trisodium Citrate and Development in Analysis Method. *AIP Conf. Proc.* **2021**, *2360*, 050007.

https://doi.org/10.1021/acsomega.2c03685
ACS Omega 2022, 7, 46066−46078